LAWRENCE
LIVERMORE
NATIONAL
LABORATORY

LLNL-JRNL-401448

On the Electronic Nature of the Surface Potential at the Vapor-Liquid Interface of Water

S. M. Kathmann, I.-F. Kuo, C. J. Mundy

February 19, 2008

Journal of the American Chemical Society

Disclaimer

On the Electronic Nature of the Surface Potential at the Vapor-Liquid Interface of Water

Shawn M. Kathmann[‡], *I-Feng William Kuo*[§], *and Christopher J. Mundy*[‡]
[‡]*Chemical and Materials Sciences Division, Pacific Northwest National Laboratory, Richland, WA 99352*

[§]*Chemical Sciences Division, Lawrence Livermore National Laboratory, Livermore, CA 94550*

The surface potential at the vapor-liquid interface of water is relevant to many areas of chemical physics. Measurement of the surface potential has been experimentally attempted many times, yet there has been little agreement as to its magnitude and sign (−1.1 to +0.5 mV). We present the first computation of the surface potential of water using *ab initio* molecular dynamics. We find that the surface potential χ = -18 mV with a maximum interfacial electric field = 8.9×10^7 V/m. A comparison is made between our quantum mechanical results and those from previous molecular simulations. We find that explicit treatment of the electronic density makes a dramatic contribution to the electric properties of the vapor-liquid interface of water. The *E*-field can alter interfacial reactivity and transport while the surface potential can be used to determine the "chemical" contribution to the real and electrochemical potentials for ionic transport through the vapor-liquid interface.

Keywords: *surface potential, electronic structure, chemical potential, electrochemistry, vapor-liquid interface*

I. Introduction

The chemistry of an ion near the vapor-liquid interface is influenced by the surface potential. Gas phase ions, even when not directly important, provide a fundamental standard state for understanding bulk and interfacial solvation. While the chemical potential is unique to each ion's identity, there is still a component of it that is both universal and fundamental to water alone – the surface potential at the vapor-liquid interface of pure water. The current study provides the most complete treatment of the spatial charge density of the vapor-liquid interface of water to date, and explains why it has been so hard to determine in the past. The surface potential χ represents the pure electrostatic potential that would exist for a unit point charge is its presence did not perturb the water structure.

The average molecular structure of the vapor-liquid interface is different from the liquid phase due to the broken symmetry provided by the interface. The electrodynamics of the vapor-liquid interface of pure water is relevant to electrochemistry, solvation thermodynamics of ions, and interfacial reactivity(1-18). The *surface potential* χ at the vapor-liquid interface of water is defined(12, 17, 18) (see Figure 1) as the difference between the liquid-phase inner "*Galvani*" potential ϕ and the vapor-phase outer "*Volta*" potential ψ and is given by

$$\chi = \phi - \psi \ . \tag{1}$$

It has not been possible to directly measure the surface potential of water(10, 11). But, indirect evidence has been used to estimate χ, however, the results do not provide a consistent sign much less the magnitude for χ (–1.1 to +0.5 mV). Pratt(11, 19) has suggested neutron scattering in conjunction with electron reflectivity experiments may

provide a more consistent picture of the structure and charge distribution of the vapor-liquid interface. The outer *Volta* potential can be determined from the work required to bring an unperturbing unit charge from infinity up to a point just outside the vapor-liquid interface. Similarly, the inner *Galvani* potential could be determined from the work required to bring an unperturbing unit charge from infinity and through the vapor-liquid interface to just inside the liquid surface. But, in practice, the work required to move a charge through an interface must involve a real physical charge i.e., an electron, or an ionic atom or molecule. The motion of a physical charge through the vapor-liquid interface is associated with changes to the interfacial structure and electronic environment. The "*electrochemical"* potential, η_i, associated with the process of moving of charged species *i* from infinity up to the surface, through the vapor-liquid interface, and then into the bulk liquid can be divided into *"chemical"*, *"real"*, and *"electrostatic"* contributions given by(12, 17, 18)

$$\eta_i = \mu_i + z_i\phi = \mu_i + z_i\chi + z_i\psi = \alpha_i + z_i\psi, \qquad (2)$$

where μ_i is the *chemical* potential, $\alpha_i = \mu_i + z_i\chi$ is the *real* potential, and z_i is the charge of the ion. Since these distinctions can be quite confusing we offer an alternative point of view: The *electrochemical* potential, η_i, can be thought of as the inhomogeneous chemical potential (in the sense of the reversible work required to move an ion between two phases), whereas the *chemical* potential, μ_i, can be thought of as the homogeneous chemical potential (i.e., the reversible work required to create an ion in a single phase). The *electrochemical* potential, η_i, and the outer *Volta* potential, ψ, can be measured directly (assuming a reference *electrochemical* potential for H^+ to be zero) yielding the

real potential α_i, however, this still leaves the *chemical* potential, μ_i, and *surface potential*, χ, (or *Galvani* potential) undetermined.

As pointed out in a review by Tobias and Jungwirth(20) and by Sokhan and Tildesley(8), molecular-level simulations hold the promise of being able to directly "measure" the surface potential χ of the vapor-liquid interface of pure water. Thus, if the surface potential χ can be calculated independently, then the chemical potential μ_i of the ion can be obtained and used in closure calculations for consistency with measurements of the electrochemical potential η_i as well as other interfacial measurements like second harmonic generation(14) or vibrational sum frequency spectroscopy(21). The surface potential χ of the vapor-liquid interface may be calculated by integrating the total interfacial electric field $E_z(z)$ across the vapor-liquid interface

$$\chi = \varphi(z_{inner}) - \varphi(z_{outer}) = -\int_{z_{outer}}^{z_{inner}} E_z(z')dz', \tag{3}$$

where $\varphi(z_{inner}) = \phi$, $\varphi(z_{outer}) = \psi$, and z is taken to be positive as one moves from the vapor to the liquid phase – the z-component is relevant since the x and y contributions sum to zero by symmetry. Similarly, the interfacial electric field is obtained by integrating the total charge density $\langle\rho(z)\rangle$, averaged over the full *ab initio* MD trajectory, across the vapor-liquid interface

$$E_z(z_{outer}) - E_z(z_{inner}) = 4\pi \int_{inner}^{outer} \langle\rho(z')\rangle dz'. \tag{4}$$

As might be anticipated, the interfacial electric field $E_z(z)$ and surface potential χ are sensitive functions of $\rho(z)$.

The central issue that is most relevant to the accurate calculation of the electrostatic potential $\varphi(z)$ as a function of z is how to represent the spatial charge density $\rho(z)$ in condensed matter. Previous studies(8, 19) and reviews(11, 20) discuss the approximation of the spatial charge density of each water molecule by a truncated multipole expansion retaining only dipole(22-25) and quadrupole terms(8). Sokhan and Tildesley(8) showed that the early studies incorporated only dipole contributions leading to the conclusion that the surface potential was positive whereas including the quadrupole contribution made the surface potential negative - see Figure 2. But, the effect of the higher multipole (octopole, hexadecapole, etc.) moments on the surface potential was not investigated(8). A multipole expansion is strictly valid(26) only when all multipole moments are included and when the test charge is located outside the spatial charge density. The spatial charge density computed from quantum mechanics includes, in principle, all multipole moments and hence does not suffer from truncation errors in the multipole expansion. Ultimately, the manner in which the charge density is distributed throughout space must be determined from quantum mechanics.

Quantum mechanics has shown that electrons are distributed throughout matter in the attractive field of the atomic nuclei – the real charge density being the sum of nuclear and electronic charges (i.e., $\rho_{tot} = \rho_{nuc} + \rho_{elec}$). However, each molecular model of water has it own particular charge distribution chosen to mimic the real charge density. The great majority of molecular models for water(27-29) employ partial point charges (δ-functions) either at the locations of the nuclei or elsewhere (e.g., patterned against the lone pair orbitals of oxygen or to produce the gas-phase dipole and quadrupole moments – see Figure 2). These water models use partial charges that are much smaller than the bare

nuclear charges because the nuclei are "screened" by the electronic charge density. Some water models include point polarizable sites(29) within the molecule in addition to the partial charges. Still fewer water models use Gaussian charge distributions centered on the nuclei with associated polarizable sites. But, in final analysis such models are idealizations of the real charge distributions of condensed phase water molecules. These idealizations are necessary because of computational limitations; however, they have served the purpose of simplifying complex phenomena in such a way as to provide useful conceptual insights. Moreover, in many cases these water models are quantitative for several properties of water with the caveat that one must exclude those properties that went into their parameterization. Table I shows a comparison of the surface potentials χ for several water models.

In recent years, the structure and electric properties of the vapor-liquid interface have received considerable attention from both experimental and theory. Experimentally, the orientational ordering of the vapor-liquid interface has been probed by second harmonic generation(14) (SHG) and sum frequency spectroscopy(21) (SFS). The interpretation of the SHG data implies that the dipole moment of water point slightly toward the liquid phase. The SFS data show the presence of free OH bonds. Sokhan and Tildesley performed molecular dynamics using the SPC/E water model to compute the surface potential, orientation, and nonlinear susceptibility. They found the surface potential for SPC/E to be χ = -546 mV at 298K. The orientational averaging revealed two distinct layers with different structures: (1) the dipoles (or C_{2v} axis) on the vapor side of the Gibbs dividing surface are tilted toward the vapor phase at an angle of 78° to the surface normal, and (2) the dipoles on the liquid side (see Figure 2) of the Gibbs dividing surface

are tilted slightly toward the liquid phase at an angle of 98° to the surface normal (other molecular studies(8, 30, 31) have found similar orientations through the interface). Their analysis of the nonlinear susceptibility showed that the two distinct layers contribute with opposite signs to the integral susceptibility with the dominant contribution coming from the liquid side of the Gibbs dividing surface i.e., where the dipole points slightly toward the liquid phase. Sokhan and Tildesley state that their surface potential χ should be considered as a lower limit due to the neglect of explicit polarization in the water model. Furthermore, they state that inclusion of polarization effects should result in an interfacial electric field that is dramatically weaker since polarization works against the inducing field. However, the polarizable water model of Dang-Chang gives a value of χ = -500 mV at 298K showing that the results for the surface potential will depend on how polarization is included. Other molecular studies(8) of the surface potential have found consistent results and are displayed in Table I for comparison.

The sensitivity of the surface potential χ has been discussed in the pioneering studies of Wilson, Pohorille, and Pratt(5, 6). They obtained a χ = -130 mV at 325K using the TIP4P model. Wilson *et al.* calculated the influence on the surface potential χ due to: (1) a modification of the TIP4P water model partial point charges (of the M-sites) into Gaussian distributions, and (2) a Gaussian fit of the electronic distribution of a single water monomer based on HF/6-31G** electronic structure data. From this study they conclude, "The surface potential is sensitive to details of the large distance wings of the molecular charge distribution."

In this paper we present *ab initio* molecular dynamics results for the surface potential χ at the vapor-liquid interface obtained directly from the total charge density $\rho_{tot} = \rho_{nuc} +$

ρ_{elec}. In sections II we discuss the methods and computational details. In section III we present the results and discussion. Finally, we close with conclusions in section IV and suggest directions for future research.

II. Methods and Computational Details

Previously(32, 33), the vapor-liquid interface was simulated using the simulation package CPMD(34) via a slab configuration containing 216 water molecule in a simulation cell of 15Å × 15Å × 71.44Å at a temperature T = 298K. A total of 7 ps was generated using the Car-Parrinello approach(35) using a time-step of 0.097 fs with a fictitious mass of 400 a.u. for the electronic degrees of freedom. The potential used was based on Kohn-Sham formulation of density functional theory where plane-waves expanded up to 70 Ry was used as the basis-set in conjunction with Martins-Troullier pseudopotentials(36) to account for the core states. Gradient corrected exchange and correlation functionals as parameterized by Becke(37) and Lee-Yang-Parr(38) was used due to its general success with hydrogen bonded systems. Individual Nosé-Hoover thermostats(39, 40) was attach to every degree of freedom with a frequency of 3800 cm^{-1} to ensure thermal equilibrium at 298K. Decoupling of periodic images in the z-direction was performed as described by Mortensen and Parrinello in conjunction with a large amount of vacuum (35 Å) to ensure convergence of surface properties.

For analysis, averaging was performed every 100 steps using the QuickStep module within CP2K(41, 42) which has been shown elsewhere that structural and dynamical properties of water are equivalent to those obtained from CPMD (42). Unlike CPMD, CP2K utilizes dual basis set of Gaussian type orbital (GTO) and plane wave basis.(43)

Specifically, we utilize a triple zeta plus double polarization (TZV2P) GTO basis and a smaller single zeta (SZV) GTO basis to test basis set dependence. For all the runs, the density was expanded up to 280 Ry for the valence states and dual-space GTH pseudopotentials (44) was used to account for the core states. It should be pointed out that it was shown that the TZV2P basis set used in this study closely reproduce the CPMD forces along identical trajectories (42). Although this cannot be said about the use of the SVP basis, it is utilized in this study to provide benchmark on the basis set effects on the value of the surface potential. The electronic states were quenched to a tolerance of 10^{-7} Hartree.

The surface potential was directly determined from the real-space electrostatic potential determined from the nuclear and electronic densities ($\rho_{tot}(\mathbf{r}) = \rho_{nuc}(\mathbf{r}) + \rho_{elec}(\mathbf{r})$ where $\mathbf{r}$ is the position vector to a point in real-space). The resulting real-space electrostatic potential is manifestly periodic through its Fourier space representation $\hat{V}_{\mathbf{g}}^{\mathrm{H}} = 4\pi\,\hat{\rho}_{\mathbf{g}}^{tot}/g^2$. Here $\hat{V}_{\mathbf{g}}^{\mathrm{H}}$ and $\hat{\rho}_{\mathbf{g}}^{tot}$ represent the Hartree potential and total density, respectively in Fourier space, and $\mathbf{g}$ represents the reciprocal lattice vectors. It is important to note that the total charge density, $\hat{\rho}_{\mathbf{g}}^{tot}$ integrates to zero indicating that we are indeed studying a neutral aqueous system. The real-space Hartree potential, $V^{\mathrm{H}}(\mathbf{r})$ is obtained by a numerical Fourier transformation of $\hat{V}_{\mathbf{g}}^{\mathrm{H}}$. $V^{\mathrm{H}}(\mathbf{r})$ is then represented in units of e^{-}/Hartree on a $N_x \times N_y \times N_z$ real-space grid with $N_x = N_y = 160$ and $N_z = 720$ determined by the density cut-off in CP2K. To obtain the electrostatic potential along the interfacial coordinate, z, a simple averaging over the x and y directions was performed, namely

$$V^{\mathrm{H}}(\mathbf{r}) \Rightarrow V_{x,y,z}^{\mathrm{H}}, \tag{5}$$

where

$$V_z^{\mathrm{H}}(z) = \varphi(z) = \frac{\sum_{x,y} V_{x,y,z}^{\mathrm{H}}}{N_x N_y}. \qquad (6)$$

The mathematical expression for the nuclear contributions is modeled as an Ewald sum in order to avoid dealing with delta-function point charges. Thus, there is an additional contribution to the electrostatic potential that is due to the overlap of the charge densities. In the present application, the overlap contribution is essentially zero (*e.g.* ~10^{-6} Hartree) and therefore not explicitly calculated.

III. Results and Discussion

The computed electrostatic potential $\varphi(z)$ is presented in Figure 3 showing the effect of two different basis sets (TZV2P and SZV). The results of the two free interfaces were averaged to produce a single surface potential profile running from the center of the simulation cell to the vacuum. Both basis sets yield very consistent results for the surface potential χ, however, the SZV results are about 1 mV smaller than the TZV2P results. The fluctuations in the surface potential observed in the liquid region are likely due to lack of adequate statistical sampling. As a self-consistent check we compared χ using the same simulation parameters and interaction potential as Wick *et al.*(31, 45) Our findings for the behavior of χ at 4-5 ps of production trajectory mimic what is observed for the sampling of the DFT liquid-vapor interface trajectory. Specifically, the fluctuations in χ using a 4 ps classical trajectory are roughly 20% of the converged value of -480 mV obtained by Wick *et al*. For the remainder of the analysis will use the surface potential results from the TZV2P basis set. The TZV2P surface potential $\varphi(z)$ data (black circles)

are shown in Figure 4 along with a tanh fit (smooth solid blue curve) to the $\varphi(z)$ data and the corresponding interfacial electric field $E_z(z)$ (dashed green curve). In Figure 4, the Gibbs dividing surface (GDS) is located at z = 9 Å (vertical dotted line). The tanh fit was performed with the function

$$\varphi(z) = c_1 \tanh(z + c_2) + c_3, \tag{7}$$

where c_1 = -8.9704, c_2 = -19.318, and c_3 = -9.0579 are constants determined by a least-squares fit. The tanh fit to the CP2K/TZV2P results yields a surface potential χ = -18 mV. Table I shows a comparison of our surface potential with those found using other water models.(8) As mentioned previously, the results, to date, from molecular simulation have uniformly found a consistent sign (negative) and magnitude for χ (hundreds of millivolts). This is consistent with the water molecules on the vapor side of the GDS having their hydrogen atoms pointing toward the vapor phase thus giving rise to the positive sign of the electric field. However, our result of χ = -18 mV is about 28 times smaller than the -500 mV found using an empirical polarizable(31, 45) interaction potential for water. It should be pointed out that although our DFT trajectory is short, our hydrogen bond populations and short time dynamics are consistent with a variety of empirical (both fixed charge and polarizable) interaction potentials.(31, 33) Moreover, as previously stated, our self-consistent check of the surface potential obtained with a short trajectory using a empirical interaction potential did not alter the average value of the surface potential. This provides strong evidence that our current trajectory contains the relevant fluctuations in structure. Thus, our computed surface potential does arise from spurious orientational structure at the interface when compared to classical water models – the dramatic difference in our surface potential must be attributed to electronic effects.

The interfacial electric field was found by numerical differentiation (centered difference) $E_z(z) = -[d\varphi(z)/dz]\hat{z}$. We obtain a maximum in the interfacial electric field $max[E_z(z)]$ = 8.9×10^7 V/m that is about 15 times smaller than the 1.4×10^9 V/m found using an empirical polarizable(31, 45) water model. Note that the interfacial electric field peaks on the vapor side of the GDS (about 1 Å to the left of the GDS in Figure 4). These results are entirely consistent with previous investigations of Pratt *et al.*, Sokhan and Tildesley, and the SHG and SFS experiments. Pratt *et al.* and Sokhan and Tildesley both indicate the importance of incorporating the appropriate charge distributions (electronic and nuclear) in the condensed phase and interfacial regions – here lies the true strength of accurate electronic structure methods. From the surface potential, the width of the interfacial region is about 5 Å. The full width at half maximum of the interfacial electric field is about 2 Å – i.e., approximately the width of a water molecule.

As mentioned previously, the determination of the surface potential χ allows the real potential $\alpha_i = \mu_i + z_i\chi$ to be partitioned into chemical (μ_i) and electric ($z_i\chi$) contributions. Using our value χ = -18 mV we find the electric contribution (for a univalent ion: $z_i = 1e$) to the real potential to be $\chi \approx 0.4$ kcal/mol/*e* which is considerably smaller than previous estimates of $\chi \approx 11.5$ kcal/mol/*e* using a typical value of χ = -500 mV. Thus, the electric contribution to the real potential utilizing a charge density obtained from electronic structure is small for the vapor-liquid interface of water.

IV. Conclusions

We have presented the first computation of the surface potential χ of water using *ab initio* molecular dynamics. Measurement of the surface potential has been

experimentally attempted many times, yet there has been little agreement as to its magnitude and sign (−1.1 to +0.5 mV). We find that the surface potential χ = -18 mV with a maximum interfacial electric field $max[E_z(z)] = 8.9 \times 10^7$ V/m. A comparison was made between our quantum mechanical results and those from previous molecular simulations underscoring the different treatment of the charge distributions (multipole expansions using dipole and quadrupole moments, partial point charges with and without polarizability, and quantum mechanical electronic structure). We find that explicit treatment of the electronic density makes a dramatic contribution to the electric properties of the vapor-liquid interface of water. The *E*-field can alter interfacial reactivity and transport while the surface potential can be used to determine the "chemical" contribution to the real and electrochemical potentials for ionic transport through the vapor-liquid interface. Future studies will address the surface potential and electric field at the interface between a salt crystal and liquid water and electronic effects on the potential of mean force of various ions through the vapor-liquid interface of water.

Acknowledgements

SMK and CJM would like to acknowledge helpful discussions with Liem Dang (PNNL), Greg Schenter (PNNL), John Daschbach (PNNL), and James Cowin (PNNL). This work was supported by the U.S. Department of Energy's (DOE) Office of Basic Energy Sciences, Chemical Sciences program and was performed in part using the Molecular Science Computing Facility (MSCF) in the William R. Wiley Environmental Molecular Sciences Laboratory, a DOE national scientific user facility located at the Pacific Northwest National Laboratory (PNNL). Part of this work was performed under the auspices of the DOE by Lawrence Livermore National Laboratory under Contract DE-AC52-07NA27344 with some computer resources being provided by Livermore Computing. PNNL is operated by Battelle for the US Department of Energy.

Figure Captions:

Figure 1. Illustration showing the connection between the outer *"Volta"* potential, ψ, the inner *"Galvani"* potential, ϕ, the *surface potential*, $\chi = \phi - \psi$, and the electric field $\vec{E}$ at the interface between the vapor (left) and liquid (right).

Figure 2. Illustration show various levels of approximation in treating spatial charge density of the water molecules at the vapor-liquid interface: a) dipole (green) and quadrupole (purple) moments, b) partial point charges, and c) electronic structure charge distribution.

Figure 3. Comparison of the electrostatic potential $\varphi(z)$ (in mV) as a function of z using two different basis sets: TZV2P (solid black) and SZV (dashed blue).

Figure 4. The TZV2P electrostatic potential $\varphi(z)$ data (black circles) along with a tanh fit (smooth solid blue curve) to the $\varphi(z)$ data and the corresponding interfacial electric field $E_z(z)$ (dashed green curve). The Gibbs dividing surface (GDS) is located at z = 9 Å (vertical dotted line).

Cover Art. Illustration of the electronic charge density at the vapor-liquid interface of water.

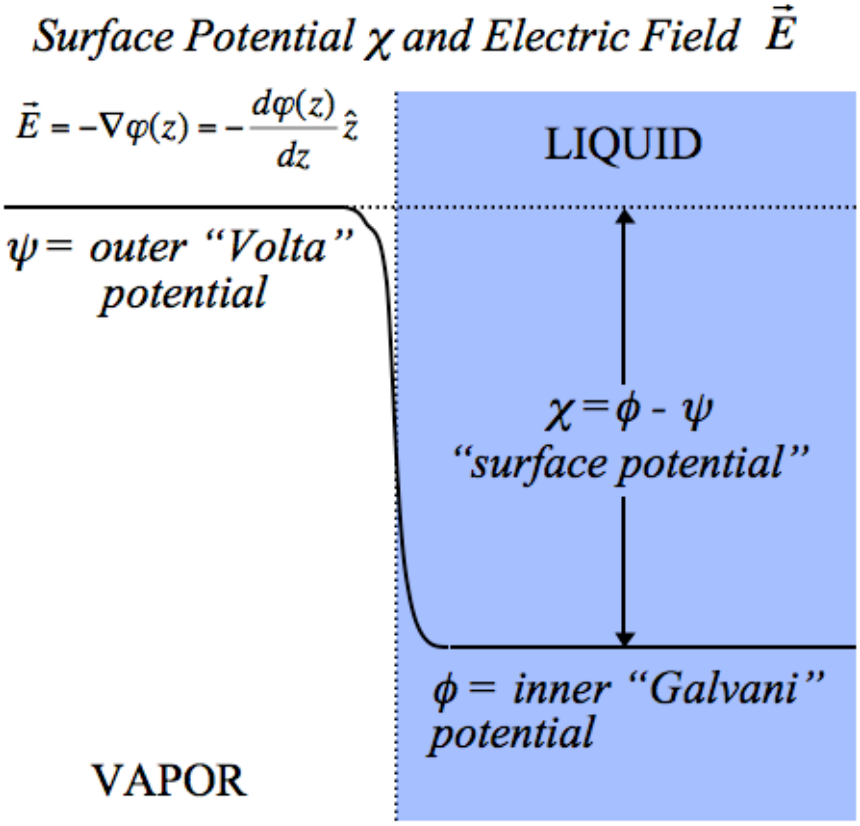
Surface Potential χ and Electric Field $\vec{E}$
$\vec{E} = -\nabla\varphi(z) = -\frac{d\varphi(z)}{dz}\hat{z}$
LIQUID
ψ = outer "Volta" potential
χ = ϕ - ψ
"surface potential"
ϕ = inner "Galvani" potential
VAPOR

Figure 1.

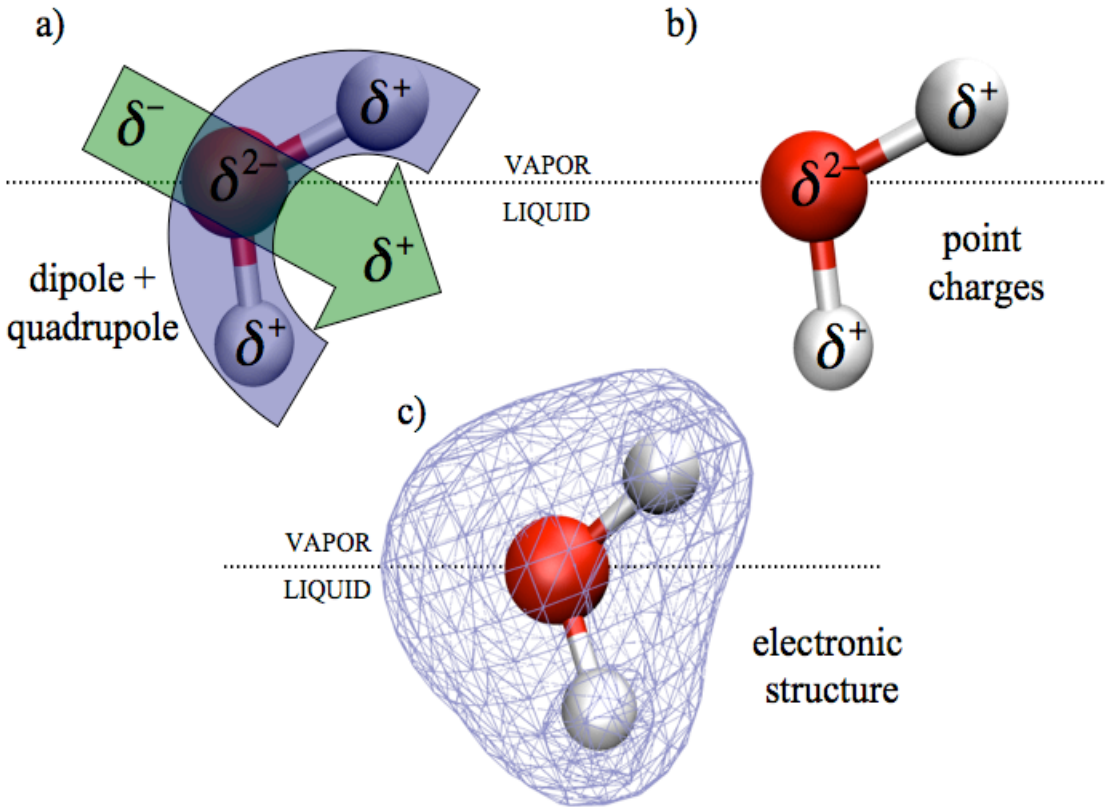
a)
b)
c)
δ−
δ2−
δ+
δ+
δ+
dipole +
quadrupole
VAPOR
LIQUID
δ+
δ2−
δ+
point
charges
VAPOR
LIQUID
electronic
structure

Figure 2.

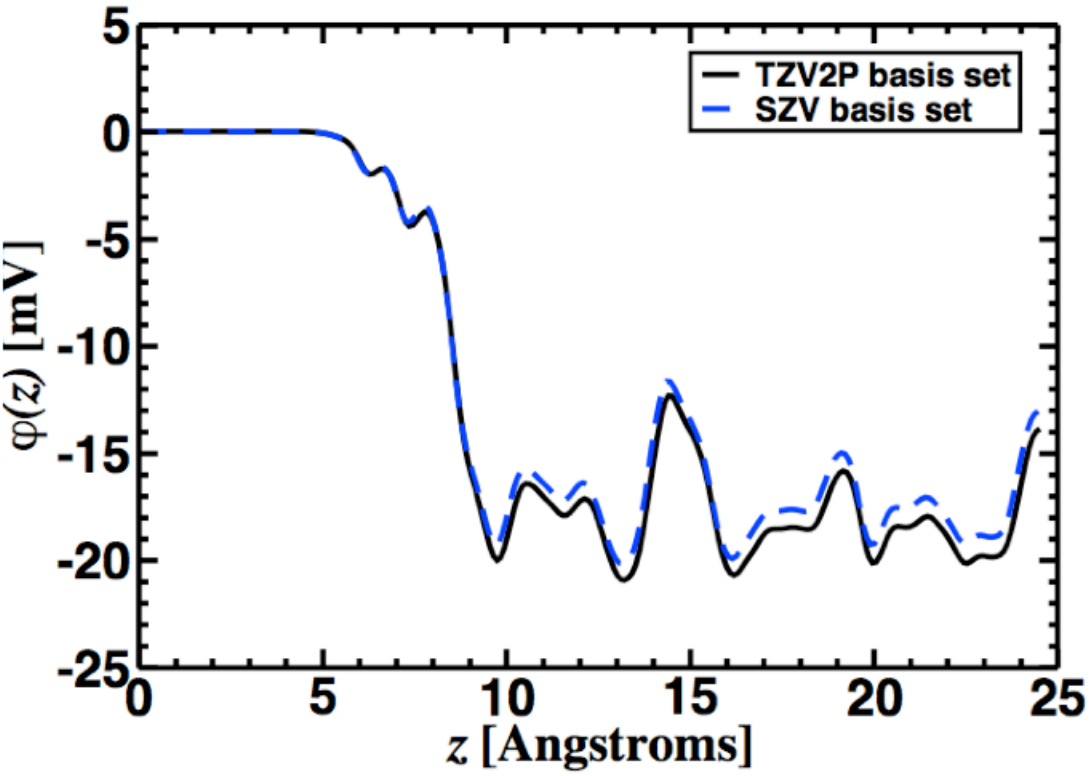
TZV2P basis set
SZV basis set
φ(z) [mV]
z [Angstroms]
5
0
-5
-10
-15
-20
-25
0
5
10
15
20
25

Figure 3.

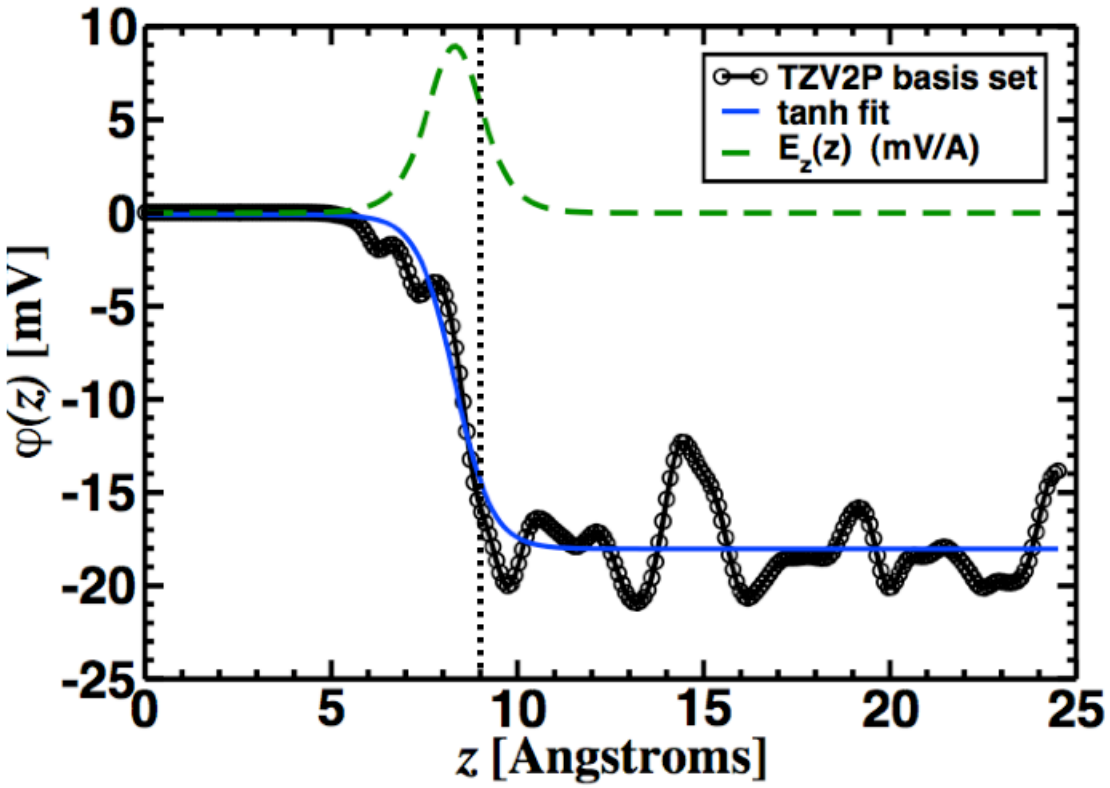
TZV2P basis set
tanh fit
E_z(z) (mV/A)
φ(z) [mV]
z [Angstroms]
10
5
0
-5
-10
-15
-20
-25
0
5
10
15
20
25

Figure 4.

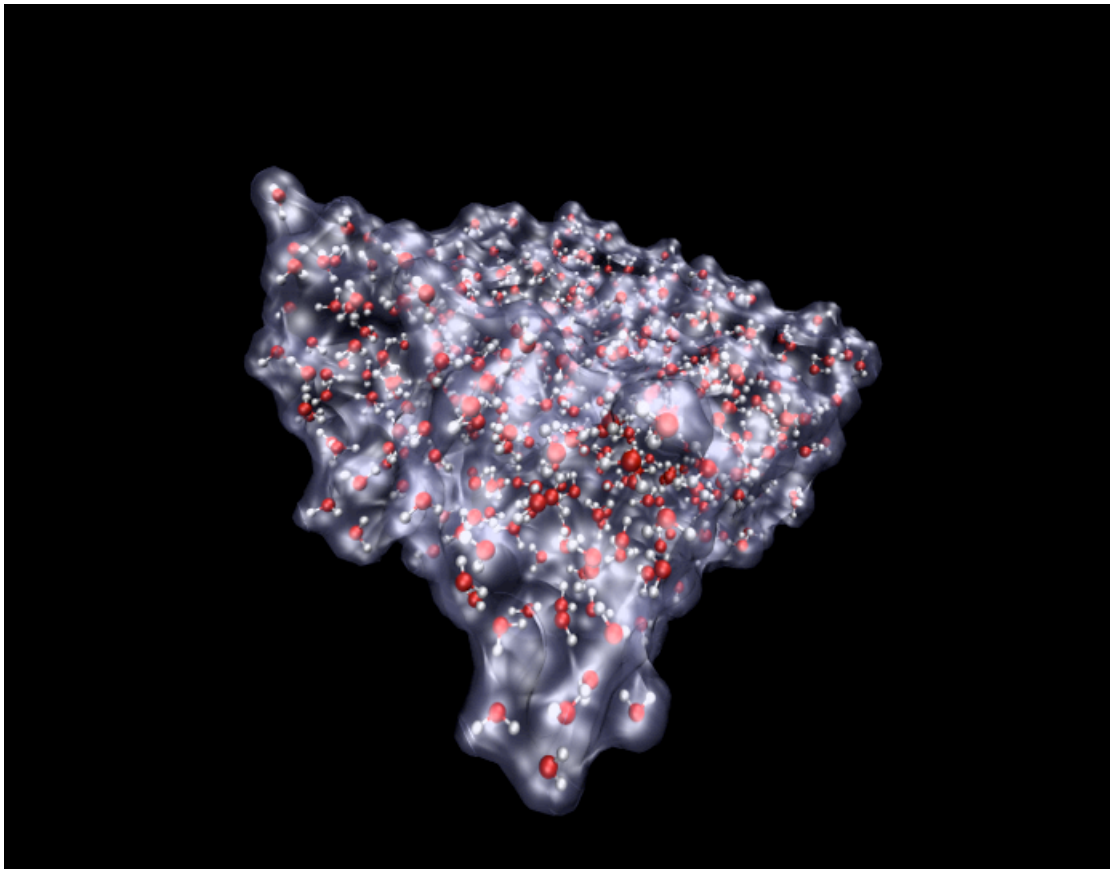

Cover Art

TABLE I. Comparison of surface potentials χ for various water models(8) at 298K. The quantum mechanical surface potential is quite different from empirical interaction potentials for water, however, the sign is consistently negative.

Water Model	χ (mV)
present study	-18
TIP4P	-510
D-C	-480
SPC/E	-546
SPC	-530
CC	-600
RWL	-530
TIPS2	-890

References

1. Motakabbir, K. A. & Berkowitz, M. L. (1991) *Chemical Physics Letters* **176,** 61.
2. Schweighofer, K. J. & Benjamin, I. (1993) *Chemical Physics Letters* **202,** 379.
3. Dang, L. X. & Chang, T.-M. (2002) *Journal of Physical Chemistry B* **106,** 235.
4. Lamoureaux, G. & Roux, B. (2006) *Journal of Physical Chemistry B* **110,** 3308.
5. Wilson, M. A., Pohorille, A., & Pratt, L. R. (1988) *Journal of Chemical Physics* **88,** 3281.
6. Wilson, M. A., Pohorille, A., & Pratt, L. R. (1987) *Journal of Physical Chemistry* **91,** 4873.
7. Stillinger, F. H. & Ben-Naim, A. (1967) *Journal of Chemical Physics* **47,** 4431.
8. Sokhan, V. P. & Tildesley, D. J. (1997) *Molecular Physics* **92,** 625.
9. Randles, J. E. B. & Schiffrin, D. J. (1965) *Journal of Electroanalytical Chemistry* **10,** 480.
10. Randles, J. E. B. (1977) *Physics and Chemistry of Liquids* **7,** 107.
11. Pratt, L. R. (1992) *Journal of Physical Chemistry* **96,** 25.
12. Koryta, J., Dvorak, J., & Kavan, L. (1993) *Principles of Electrochemistry* (John Wiley & Sons, New York).
13. Gomer, R. & Tryson, G. (1977) *Journal of Chemical Physics* **66,** 4413.
14. Goh, M. C., Hicks, J. M., Kemnitz, K., Pinto, G. R., Bhattacharyya, K., Eisenthal, K. B., & Heinz, T. F. (1988) *Journal of Physical Chemistry* **92,** 5074.
15. Farrell, J. R. & McTigue, P. (1982) *Journal of Electroanalytical Chemistry* **139,** 37.

16. Eley, D. D. & Evans, M. G. (1938) *Transactions of the Faraday Society* **XXXIV,** 1093.

17. Bard, A. J. & Faulkner, L. R. (1980) *Electrochemical Methods: Fundamentals and Applications* (John Wiley & Sons, New York).

18. Adamson, A. W. (1990) *Physical Chemistry of Surfaces* (John Wiley & Sons, New York).

19. Parfenyuk, V. I. (2002) *Colloid Journal* **64,** 588.

20. Jungwirth, P. & Tobias, D. J. (2006) *Chemical Reviews* **106,** 1259.

21. Richmond, G. L. (2002) *Chemical Reviews* **102,** 2693.

22. Aloisi, G., Guidelli, R., Jackson, R. A., Clark, S. M., & Barnes, P. (1986) *Journal of Electroanlytical Chemistry* **206,** 131.

23. Christou, N. I., Whitehouse, J. S., Nicholson, D., & Parsonage, N. G. (1985) *Molecular Physics* **55,** 397.

24. Matsumoto, M. & Kataoka, Y. (1988) *Journal of Chemical Physics* **88,** 3233.

25. Barraclough, C. G., McTigue, P. T., & Ng, Y. L. (1992) *Journal of Electroanalytical Chemistry* **329,** 9.

26. Jackson, J. D. (1962) *Classical Electrodynamics* (John Wiley & Sons, New York).

27. Berendsen, H. J. C., Grigera, J. R., & Straatsma, T. P. (1987) *Journal of Physical Chemistry* **91,** 6269.

28. Jorgensen, W. L., Chandrasekhar, J., Madura, J. D., Impey, R. W., & Klein, M. L. (1983) *Journal of Chemical Physics* **79,** 926.

29. Dang, L. X. & Chang, T.-M. (1997) *Journal of Chemical Physics* **106,** 8149.

30. Taylor, R. S., Dang, L. X., & Garrett, B. C. (1996) *Journal of Physical Chemistry* **100,** 11720.

31. Wick, C. D., Kuo, I.-F. W., Mundy, C. J., & Dang, L. X. (2007) *Journal of Chemical Theory and Computation* **3,** 2002.

32. Kuo, I. F. W. & Mundy, C. J. (2004) *Science* **303,** 658-660.

33. Kuo, I. F. W., Mundy, C. J., Eggimann, B. L., McGrath, M. J., Siepmann, J. I., Chen, B., Vieceli, J., & Tobias, D. J. (2006) *Journal of Physical Chemistry B* **110,** 3738-3746.

34. CPMD (http://www.cpmd.org).

35. Car, R. & Parrinello, M. (1985) *Physical Review Letters* **55,** 2471.

36. Troullier, N. & Martins, J. L. (1991) *Physical Review B* **43,** 1993.

37. Becke, A. D. (1988) *Physical Review A* **38,** 3098.

38. Lee, C., Yang, W., & Parr, R. G. (1988) *Physical Review B* **37,** 785-789.

39. Nose, S. (1984) *Journal of Chemical Physics* **81,** 511-519.

40. Hoover, W. G. (1985) *Physical Review A* **31,** 1695.

41. CP2K (http://cp2k.berlios.de).

42. VandeVondele, J., Krack, M., Mohamed, F., Parrinello, M., Chassaing, T., & Hutter, R. (2005) *Computer Physics Communications* **167,** 103-128.

43. Lippert, G., Hutter, J., & Parrinello, M. (1997) *Molecular Physics* **92,** 477.

44. Goedecker, S., Teter, M., & Hutter, J. (1996) *Physical Review B* **54,** 1703.

45. Wick, C. D., Dang, L. X., & Jungwirth, P. (2006) *Journal of Chemical Physics* **125,** 024706.